

Cryogenic Target Characterization: Over the past year, 31 cryogenic targets of $\sim 900\text{-}\mu\text{m}$ o.d., $5\text{-}\mu\text{m}$ wall, filled with approximately ~ 1000 atm of D_2 , and cooled to ~ 18 K have been produced, characterized, and shot at LLE. The characterization is based on shadowgraphy (DOE Monthly Progress Report, March 2003), and software tools have been created to analyze these data for surface and ice-thickness variations. A typical result of a shadowgram of a cryogenic target is shown in Fig. 1(a). The outermost bright ring inside the target surface is representative of the ice layer. The breaks in the ring are caused by either outer-surface imperfections or ice nonuniformities.

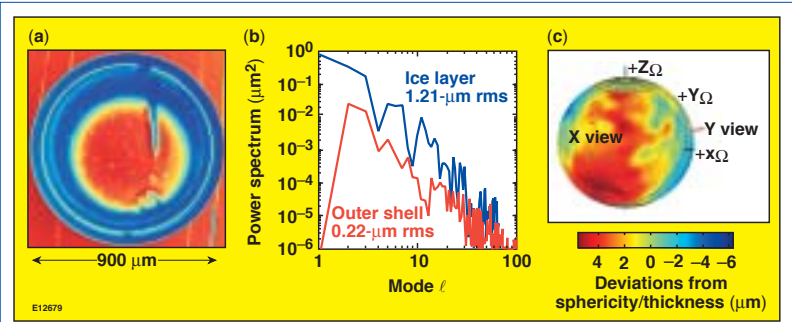


Figure 1. Shadowgram of a cryogenic target with an $\sim 100\text{-}\mu\text{m}$ ice layer (a). Average power spectra of outer target surface and ring due to the ice layer (b). Three-dimensional view of ice-layer-thickness variations obtained from a large number of shadowgrams taken from the x-viewing direction (c).

These data are unfolded to form a rectangular image in radius ($\sim 100\text{-}\mu\text{m}$ band) and angle (360°). Breaks in the ring or surface problems (e.g., tangent spider silks) are appropriately interpolated. As many as 30 shadowgrams are taken at different angles, and average power spectra of the ice surface variations are generated using FFT's. An average power spectrum is shown in Fig. 1(b) corresponding to the target in Fig. 1(a). The same shadowgrams are collated to form a three-dimensional image of the ice-layer thickness shown in Fig. 1(c). The ice-thickness variations are shown in color (see colorbar). The ice thickness can be calculated from the location of the bright ring in the shadowgram as well as from the D_2 -fill pressure. The two independent measurements agree to within 3%, which is considered to be excellent agreement. Due to the viewing angles, there are dead zones near the poles where no data are collected.

The shadowgraphic technique has been analyzed using a 1-D ray-trace simulation and a 3-D optics code (courtesy of Prof. Thomas Brown, The Institute of Optics). The former gave precise information about the locations and origins of the many different rings that may be observed. By contrast, the optics code was used to understand the importance of outer-surface perturbations on perceived inner-ice-surface perturbations. Figure 2 shows simulated bright-ring positions for a target with a perfect outer surface and a perturbed inner ice layer. The ice-layer perturbations are fully measurable in this case (a). For a perturbed outer surface and a perfect ice layer, the ring may or may not be distorted depending on the exact location of the outer-surface perturbations [(b) and (c)]. This demonstrates that outer-surface perturbations must be kept small compared to the expected inner-ice-surface perturbations. It also confirms observations where small outer-surface perturbations or miniscule dust particles may lead to partial or complete disruptions of the ring.

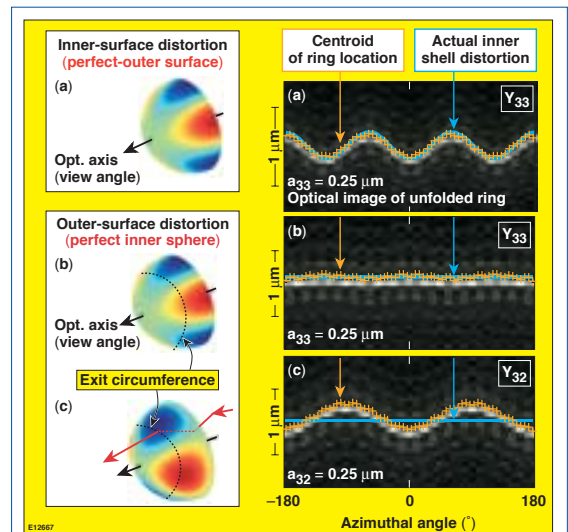


Figure 2. Results obtained with a 3-D optics imaging code for a perfect outer target surface with inner-ice-layer perturbations (Y_{33} with $0.25\text{-}\mu\text{m}$ amplitude) (a). The inner-ice-surface perturbations are easily measurable. Outer surface perturbations may cause apparent ice-surface perturbations as shown in (b) and (c), depending on their location.

OMEGA Operations Summary: OMEGA completed 94 target shots during the month of September: 29 shots for LLE [10 for RTI experiments, 3 for the power-balance campaign, 12 for the SSP program, 2 for cryo experiments, and 2 for ISE experiments]; 19 shots for LLNL; and 46 shots for LANL. The second week of September was dedicated to scheduled maintenance highlighted by the creation of the EP entrance hole in the Target Bay wall; the installation of a new diode-pumped regenerative amplifier on the SSD driver (to replace the prototype diode-pumped regenerative amplifier); improvements to the SSD-driver near-field spatial profile; the relocation of the ASBO laser to the Target Bay; and completion of the effort to recoat OMEGA's 60 primary pickoffs (to eliminate scatter).

to replace the prototype diode-pumped regenerative amplifier); improvements to the SSD-driver near-field spatial profile; the relocation of the ASBO laser to the Target Bay; and completion of the effort to recoat OMEGA's 60 primary pickoffs (to eliminate scatter).